J. Fluid Mech. (1980), *vol.* 96, *part* 1, *pp.* 65–80
Printed in Great Britain

The gravitational collapse of a mixed region into a linearly stratified fluid

By R. AMEN AND T. MAXWORTHY†

Department of Aerospace Engineering,
University of Southern California, Los Angeles

(Received 20 October 1978 and in revised form 14 June 1979)

A theoretical and experimental investigation of the collapse of a mixed region into a linearly stratified fluid is presented. An analytical model is developed for the motion of the nose of the mixed region, valid for small dimensionless times and it compares well with the experimental results of the present study and previous investigators. For longer times the length of the mixed region did not increase as the square root of the dimensionless time, as previously reported (Wu 1969), for an aspect ratio (half the initial vertical extent divided by the initial horizontal extent) equal to one. In our experiments the length did increase as a power of the dimensionless time also, but with values of the exponent between 0·89 and 0·38, depending on the values of the various parameters. It is concluded that the motion cannot be described by a simple quasi-steady buoyancy–inertia balance only. We argue that the production of internal solitary waves and their interaction with the mixed region are critical to a complete understanding of the experimental results.

1. Introduction

Mixed region collapse occurs naturally in both the oceans and the atmosphere. For example, in the ocean the mixed region may be produced by breaking internal waves, upwelling, wave–wave interactions, tidal mixing along coastlines and over topographic features and shear and frontal instabilities, to name a few. The region then has an excess of potential (and perhaps kinetic) energy over its surroundings and seeks to equilibrate rapidly. As it does so, internal waves are produced and mixed fluid is carried along the isopycnals.

Interest in this process was initiated by a study of wakes of bodies of revolution travelling in the oceanic thermocline by Schooley & Stewart (1963), who performed an experiment on the disturbances created by self propelled bodies in a stratified fluid. As a body of revolution moves through the thermocline the propeller and the flow over the body mixes the fluid into a momentumless wake. Close to the body the wake grows in the vertical and horizontal directions. However, further downstream as the turbulent energy decays, buoyancy inhibits further vertical growth and the wake collapses, growing in the horizontal direction and generates internal waves as it does so. Further experiments were performed by Schooley & Hughes (1972) and Merritt

† Also Department of Mechanical Engineering, University of Southern California.

0022-1120/80/4388-8030 $02.00

(1974) who found that after the initial collapse that $L/L_0 \simeq C_1(tN)^{\frac{1}{2}}$† for $tN < 6{\cdot}3$ and thereafter $L/L_0 \simeq C_2(tN)^{\frac{1}{3}}$.

In order to model the collapse process in a more controlled manner Wu (1969) released a two-dimensional, quiescent, cylindrical mixed region into a linearly stratified fluid. He suggested that the collapse occurred in three stages. The initial stage was characterized by a constant acceleration of the nose of the mixed region and ended before $tN = 3{\cdot}0$. The second or principal stage then began and by $tN \simeq 25$ the final stage was reached in which the nose of the mixed region moved so slowly that viscous forces became important in the over-all force balance. He found that the collapse during the initial stage can be expressed as $(L-L_0)/L_0 = c_1(tN)^{m_1}$ and during the principal stage as $L/L_0 = c_2(tN)^{m_2}$. The empirical constants were found to be: $c_1 = 0{\cdot}29(\pm 0{\cdot}04)$, $m_1 = 1{\cdot}08(\pm 0{\cdot}05)$, $c_2 = 1{\cdot}03(\pm 0{\cdot}05)$, $m_2 = 0{\cdot}55(\pm 0{\cdot}02)$ and the wave energy produced was found to peak at $0{\cdot}8N$. This result suggests that the principal stage of motion represents an instantaneous buoyancy–inertia balance.

Numerous theoretical models have been proposed to explain these rather limited results. Hartman & Lewis (1972) used a linear analysis to describe the initial motion of a partially mixed region while Hindman (1974) included the effects of viscosity in order to remove the difficulties found in this solution. These results and those of Kao (1976) and Pao (1974) predict that the horizontal extent of the mixed region should increase as $(tN)^2$. Bell & Dugan (1974) obtained both an 'exact'‡ and an asymptotic solution for a model of the collapse at small times. In the exact solution a similarity assumption was invoked and the pressure was assumed constant across the interface between the region and the ambient fluid and an energy balance argument was used to obtain a solution for the motion of the nose of the mixed region. Both solutions have been plotted in figure 3. Dugan, Warn-Varnas & Piacsek (1976) then extended this solution by assuming that the kinetic energy is shared equally by the flow in the mixed region and the external flow field.

Using a theory originally developed to describe the motion of a gravity current Kao (1976) derived the time dependence of the motion of the nose of the mixed region during the principal stage, while Manins (1976*b*) assumed that the motion maintains an instantaneous balance between buoyancy and horizontal inertia forces, as is also found in steady intrusive motions (see Manins 1976*a*). In both these investigations it was predicted that the dimensionless horizontal extent of the mixed region should be proportional to $(tN)^{\frac{1}{3}}$ for the principal stage. Several different numerical solutions have been attempted [see, for example, Wessel (1969), Young & Hirt (1972), Dugan *et al.* (1976)], while only the latter appears to be free of any serious criticism and agrees reasonably well with the limited number of experimental results.

More recently Maxworthy (1980) in a series of experiments using more realistic density distributions has found a parameter range in which the leading edge of the mixed region is trapped within a large amplitude solitary wave generated by the initial collapse. As a result, the horizontal extent of the mixed region increases linearly with time, a situation that we also consider to be a possible limit for the flows presented in this paper.

† Here N $(= [-(g/\rho)\,\partial\rho/\partial z]^{\frac{1}{2}})$ is the intrinsic frequency of the ambient stratification, L and L_0 the horizontal extent of the collapsing mixed region and its initial value, respectively.

‡ Bell and Dugan (1974) called their solution exact in that their model yielded an exact solution to the problem proposed by Mei (1969).

Since the initial interest in mixed regions produced by mechanical means, the collapse phenomenon has been considered as a mechanism contributing to the fine-scale structure of the oceanic thermocline. Maxworthy & Browand (1974) and Long (1970) have added credibility to this argument. The thermocline is characterized by a step structure with regions of high density and velocity gradient (sheets: Woods, 1968) separating regions of little or no density gradient (layers). As one possible mechanism, consider breaking internal waves travelling on a sheet, as proposed by Long (1970) or a local shear instability (Maxworthy & Browand 1974). The fluid would mix locally owing to turbulence and the mixed blob of fluid would find itself with an excess of potential energy and then collapse. This could contribute to the formation of another sheet-layer structure, possibly of finer scale, as well as internal waves. It is the application of the collapse process to such oceanic and atmospheric phenomena that motivated the present study.

In the present theoretical and experimental investigation we hope to further the understanding of this very complex phenomenon. In § 2 we present an extension of the Bell & Dugan (1974) analysis of the initial motion, in § 3 the apparatus, in § 4 the results and in § 5 a discussion of these results and their implication for motions in natural systems.

2. Theoretical solution for small times after release

In the present experiment when the dam is removed or in the case of a collapsing wake when the wake ceases to grow vertically, the mixed region begins to expand in the horizontal direction. The start of this motion is characterized by large accelerations of the fluid particles and the applicable equations of motion are nonlinear and do not lend themselves to a simple analytical solution. During this period the motion is represented by a balance between buoyancy and inertial forces so that the potential energy that was added to the system by mixing is transformed primarily into kinetic energy. If the Reynolds number associated with the flow is high enough an inviscid model should describe the motion of the collapsing mixed region. An initial Reynolds number may be defined as

$$Re_0 = NL_0^2/\nu,$$

where N is the buoyancy frequency, L_0 is the initial horizontal extent of the mixed region and ν is the kinematic viscosity of the fluid. For the experiment of Wu (1969) this number ranges from $5{\cdot}9 \times 10^3$ to 4×10^4 while in the present experiment the range is from $5{\cdot}7 \times 10^3$ to $1{\cdot}2 \times 10^4$. For the first few buoyancy oscillation periods then, the motion may be considered inviscid.

A model of the initial motion of the collapse is developed using an inviscid similarity solution. The flow in the mixed region is modelled by a quasi-steady stagnation point flow after Bell & Dugan (1974) but because their solution accelerates much faster than the experimental data we include the effects of motion in the external field as the next step in refining the model. The simplest flow field that satisfies our requirements is that of a quadrupole since the fluid must move horizontally in front of the advancing nose (cf. Browand & Winant 1972) and vertically at the upstream wall. The use of a quadrupole is further supported by the numerical solution of Young & Hirt (1972). The mixed region is assumed to be elliptic in shape and the exterior

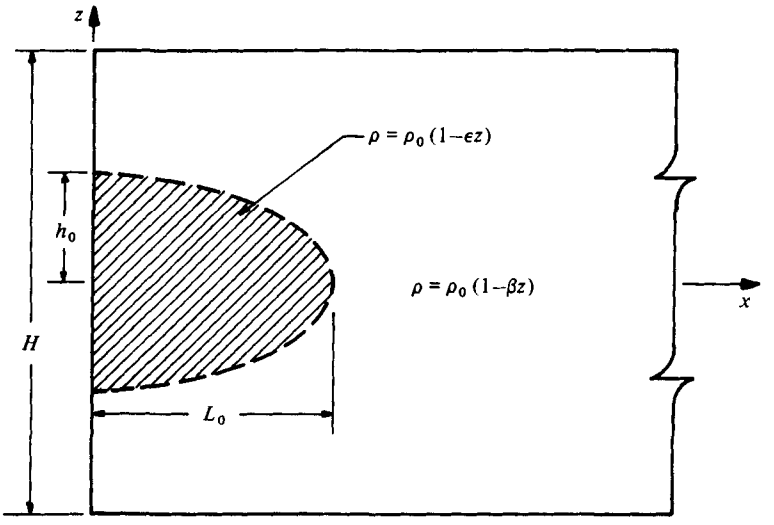

FIGURE 1. Theoretical model for an elliptically shaped region of linearly stratified fluid collapsing into an ambient linear stratification of different scale height.

region to be finite in vertical extent (see figure 1). Both the aspect ratio of the mixed region ($A = h_0/L_0$) and the depth ratio ($\phi = h_0/H$) enter into the model equation as parameters. The assumption of an elliptical shape is reasonable even for the initially rectangular region of the present experiment, since as can be seen in the photographs of two experiments (figures 6–8, plates 1 and 2), the rectangular region quickly deforms into this shape and looks identical to Wu's (1969) experiment which started out semi-cylindrical in form.

The method used to obtain the model equation is to compute the potential and kinetic energies of the flow fields and perform an energy balance following Bell & Dugan (1974). In keeping with the Boussinesq approximation, differences in density are ignored except when they give rise to buoyancy forces. The kinetic and potential energies of the mixed region are derived in an identical manner to Bell & Dugan (1974) except for the inclusion of A and ϕ and will not be considered in detail here. Then the internal kinetic and potential energies are given by

$$T_i = \tfrac{1}{16}\rho_0\pi(dL/dt)^2 L_0 h_0(1 + L_0^2 h_0^2/L^4), \tag{2.1}$$

$$U_i = \tfrac{1}{16}\rho_0\pi N^2(1-\eta L/L_0)^2 h_0^3 L_0^3 L^{-2}, \tag{2.2}$$

where $\eta = \epsilon(0)/\beta$ is a mixing parameter, $\epsilon(t)$ and β are the interior and exterior density gradients, respectively (see figure 1).

For the external flow the complex potential of a quasi-steady quadrupole is given by $W_e = Q(t)/\zeta^2$, where $Q(t)$ is the quadrupole strength and is to be determined by matching velocities at the boundary of the mixed region. The kinetic energy of the external fluid is given by

$$T_e = 2Q^2\rho_0 \int_{-\frac{1}{2}\pi}^{\frac{1}{2}\pi} \int_{B(\theta)}^{H(\theta)} r^{-5}\, dr\, d\theta,$$

where a transformation to polar co-ordinates has been made to simplify the integration. Here $B(\theta) = Lh/(L^2\sin^2\theta + h^2\cos^2\theta)^{\frac{1}{2}}$ is the boundary of the mixed region and

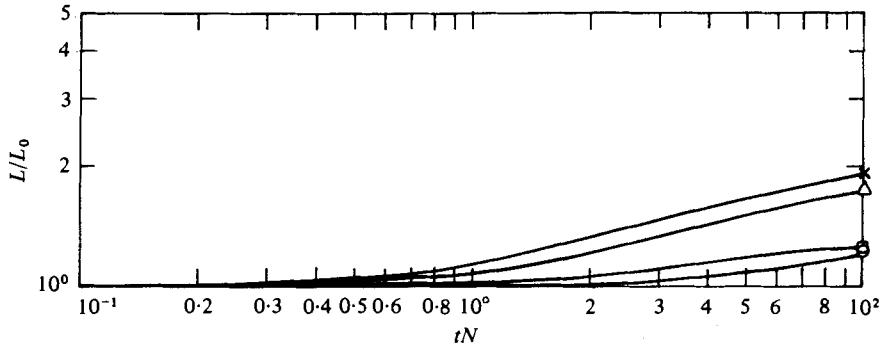

FIGURE 2. Theoretical results for the following conditions: ×—×, $\eta = 0, A = 1$; △—△, $\eta = 0{\cdot}5$, $A = 1$; □—□, $\eta = 0{\cdot}9$, $A = 1$; ○—○, $\eta = 0, A = 0{\cdot}5$.

$H(\theta) = H/\sin\theta$ is the boundary of the thermocline (or experimental tank). After integration, the external kinetic energy becomes:

$$T_e = \frac{\rho_0 \pi}{32}\left(\frac{dL}{dt}\right)^2\left[\frac{L^6}{L_0^2 h_0^2} + \frac{3}{2}\left(L^2 + \frac{L^{10}}{L_0^4 h_0^4} - \frac{L^6}{H^4}\right)\right]. \tag{2.3}$$

It should be noted here that placing a single quadrupole at the origin does not satisfy exactly the condition that there be no normal velocity across the top and bottom of the thermocline. In order to satisfy this condition, an infinite series of quadrupoles above and below the thermocline would be needed and, as a result, the algebra soon becomes unwieldy. We feel that because of the simplifying assumption made already, the extra effort required to satisfy this condition is not warranted.

The next step would be to compute the change in the potential energy of the fluid external to the mixed region. However this soon becomes such a complex expression that we have ignored this step and have only considered the modification to the Bell & Dugan (1974) solution created by the addition of a kinetic energy change in the external field. We also note that the numerical solution of Dugan *et al.* (1976) suggests that very little potential energy is stored in the external fluid during the initial collapse and can be reasonably neglected. Let $\alpha = L/L_0$ and $\tau = tN$. Collecting terms in the form of an energy balance yields:

$$\dot{\alpha}^2[A + A^3\alpha^{-4} + \tfrac{1}{2}A^{-2}\alpha^6 + \tfrac{3}{4}(\alpha^2 + A^{-4}\alpha^{10} - A^{-4}\phi\alpha^6)] + (1-\eta\alpha)^2 A^3\alpha^{-2} - (1-\eta)^2 A^3 = 0. \tag{2.4}$$

The condition that the velocity be zero and $L = L_0$ at $t = 0$ has been used to evaluate the constant arising from the energy balance.

The model equation has been numerically integrated. Typical results of the computations are plotted in figure 2 where we plot the solution to the model equation for aspect ratio equal to 1·0, depth ratio equal to 0·3 and three values of the mixing ratio. Also included is a plot for the mixing ratio equal to zero (fully mixed), depth ratio equal to 0·3 and aspect ratio equal to 0·5. The depth ratio was chosen to be 0·3 because this value matches the average depth ratio of the our earlier experiments. The solution is very sensitive to the aspect ratio and for the case of aspect ratio equal to 0·25 there is almost no motion at all. This is probably caused by an over estimation of kinetic energy in the external field since the condition of zero velocity across the top and

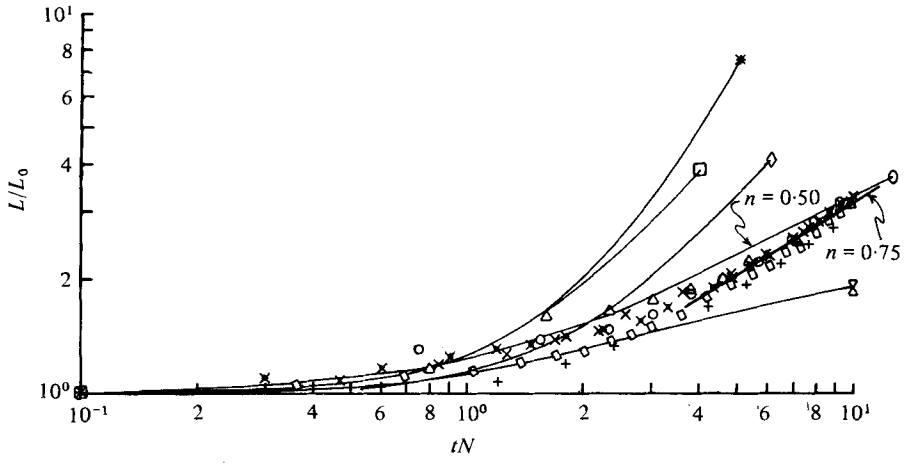

FIGURE 3. L/L_0 *vs.* tN for $A = 1$, $\phi = 0{\cdot}3$ and various N. Comparison with theory and data of Wu (1969): *—*, Bell & Dugan (1974) (asymptotic results); □—□, Bell & Dugan (1974) (exact result); ○—○, Wu (1969); ⧖—⧖, present results; ◇—◇, Dugan *et al.* (1976).

bottom of the thermocline has not been satisfied. From equation (2.3) it can be seen that owing to the dependence on L, the external kinetic energy increases for decreasing aspect ratio.

Finally the solution for aspect ratio equal to 1·0, depth ratio equal to 0·3 and mixing ratio equal to 0·1 is plotted in figure 3 along with the solutions of Bell & Dugan (1974), Dugan *et al.* (1976), data from the present experiment and the averaged data of Wu (1969). The analytic result of Dugan *et al.* (1976) appears to compare well for some range of tN during the initial stage of collapse. Their solution indicates a higher acceleration of the tip of the mixed region than has been seen in the present experiments and those of Wu (1969). The *a priori* assumption of Dugan *et al.* (1976) that the kinetic energy was equipartitioned between the interior and exterior regions was obtained from a rather tenuous interpretation of their numerical results [which did not compare well with Wu's (1969) experiment for small dimensionless times]. The present similarity solution attempts to extend the work of Bell & Dugan (1974) with an *a priori* assumption regarding the character of the external flow based on experimental observations. For aspect ratio equal to one the solution compares well to about $tN = 2{\cdot}5$ and is within the experimental accuracy.

3. Apparatus and experimental procedure

The majority of the experiments were carried out in a $30 \times 24 \times 12$ m plexiglass tank, while some of the earlier experiments were carried out in a tank of the same cross-section 5 m long. The working fluid was salt water, stratified linearly using the method introduced by Oster (1976). The salt was mixed with water in a mixing tank prior to filling the experimental tank (see figure 4) with the initial density in the mixing tank the largest desired. As fluid was drawn out of the mixing tank, fresh water was introduced at half the withdrawal rate. A floating diffuser in the experimental tank ensured that the incoming solution mixed very little as the tank filled.

A wave trap was installed at the downstream end of the experimental tank to

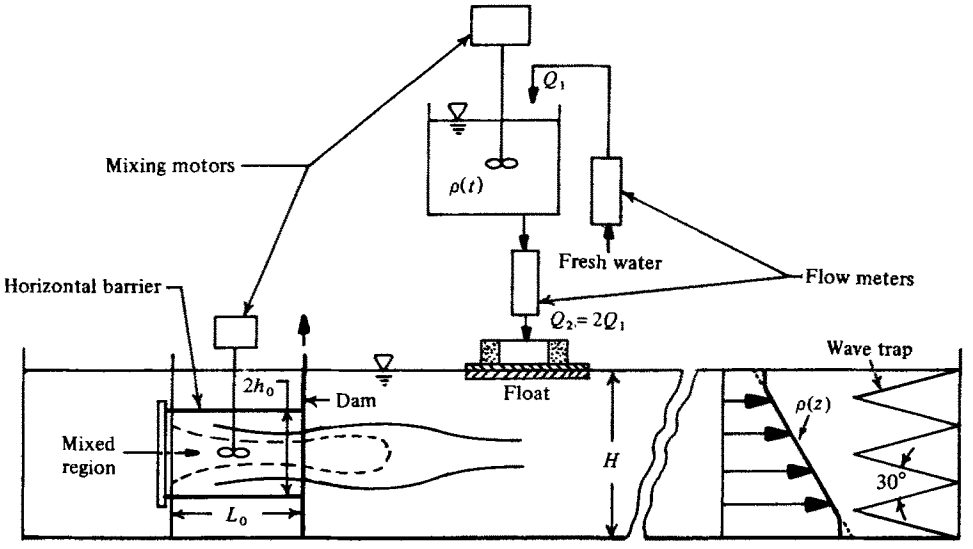

FIGURE 4. Apparatus, showing the method of producing a linear stratification and of producing the initial mixed region.

absorb energy from the internal waves. The angle of the 'beaches' of the trap was computed to absorb waves of frequency $\omega/N \geqslant 0{\cdot}2$. As mentioned earlier, Wu (1969) found that the wave energy due to the collapse process was peaked at frequencies of $0{\cdot}8N$ and that at frequencies equal to about $0{\cdot}2N$ the energy density was less than 15% of the maximum. Wunsch (1968) reported that internal waves incident on a sloping beach will be totally absorbed when their frequency $\omega/N \geqslant \sin\beta$, while waves of frequency $\omega/N < \sin\beta$ will be totally reflected (here β is the beach half angle). Although the wave trap did not completely absorb all the wave energy, it was observed that the waves reflected from the wave trap were of higher mode and travelled slower than the incedent wave. To observe this, potassium permanganate crystals were dropped into the tank near the wave trap before and just after the wave had reached the trap. The length of the tank did, however, prevent the reflected wave energy from influencing the collapse process until after the final decay stage was reached.

The mixed region was made by blocking off a portion of one end of the tank with a vertical partition and at the same time inserting two pieces of plexiglass horizontally into this region (see figure 4). These horizontal barriers limited the vertical extent of mixing. A small motor-driven propeller was inserted into the fluid through a hole in the top horizontal barrier. After the mixing was completed and the region had returned to a quiescent state the horizontal barriers were withdrawn. The experiment was started by quickly and smoothly pulling the dam vertically from the tank.

The horizontal and vertical extents of the mixed region, as well as the elapsed time, were recorded photographically. The time of arrival of the first internal wave at downstream stations was also recorded photographically, using potassium permanganate traces to mark the flow and in one experiment a conductivity probe was used to observe the waves produced by the collapse.

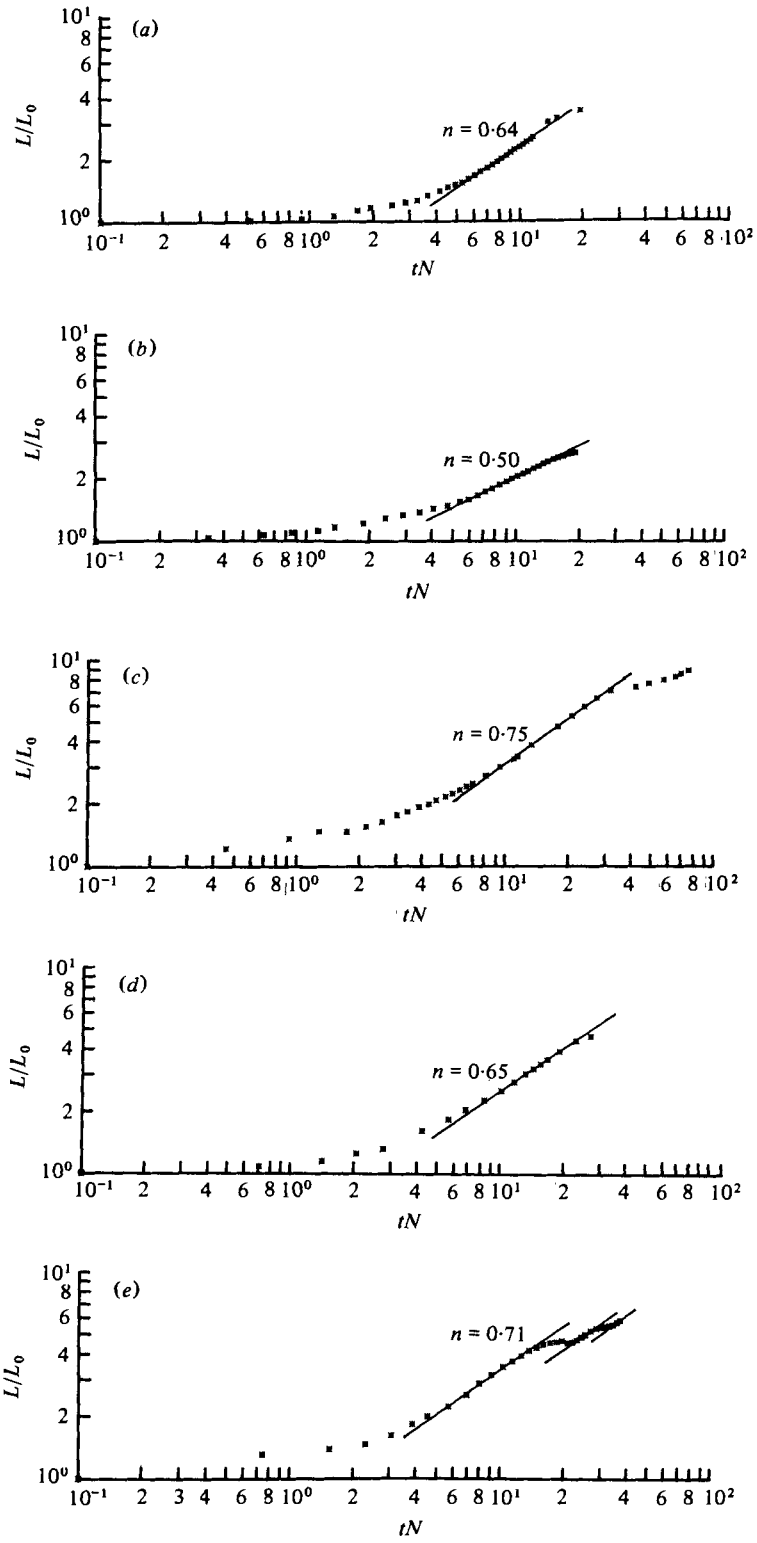

FIGURE 5. For legend see facing page.

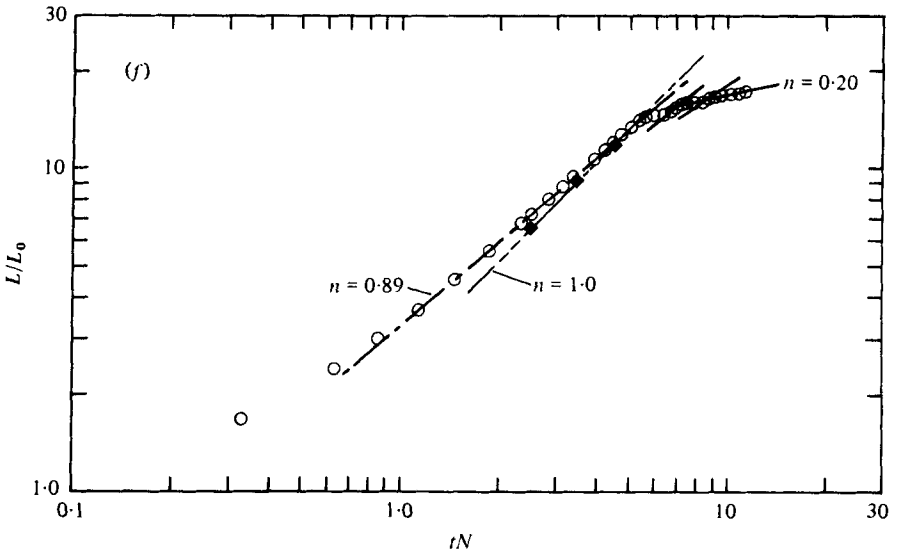

FIGURE 5. Experimental results of L/L_0 *vs.* tN for several values of N, ϕ and A. (*a*) Run 82: N = 1·30 rad/s, A = 0·29, ϕ = 0·30. (*b*) Run 117: N = 0·57 rad/s, A = 0·33, ϕ = 0·22. (*c*) Run 97: N = 0·92 rad/s, A = 0·56, ϕ = 0·34. (*d*) Run 103: N = 1·17 rad/s, A = 0·59, ϕ = 0·38. (*e*) Run 105: N = 1·15 rad/s, A = 1·0, ϕ = 0·36. (*f*) Run 170: N = 0·97 rad/s, A = 1·0, ϕ = 0·5. —○—, motion of nose-tip; —◆—, motion of central bulge of mixed region (n = 1·0).

4. Experimental results

The data for six typical experiments are presented in figure 5. The plotted data have been corrected for parallax and made dimensionless using L_0 and N. The beginning and end of the principal stage of the collapse along with the slope of the log L/L_0 *vs.* log tN curve (or exponent, n) is presented in table 1. The slopes of the principal stage of the log L/L_0 *vs.* log tN curves (figures 5*a–f*) were computed using a linear least squares fit. It should be noted that the exponent thus computed will be effected by only an insignificant amount by changes in the dimensionless times due to errors in the time of dam removal (this is true of Wu's (1969) experiment also). Of particular interest is the observation that the exponent for the A = 1 data is not $\frac{1}{2}$ as was suggested by Wu (1969) and others (see also figure 3). The average exponent for this aspect ratio varies between 0·75 and 0·89 depending on the value of ϕ. The peculiar pulsed characteristic of the L/L_0 *vs.* tN history for the larger values of ϕ and A (e.g. figure 5*e*) is of great interest and can be explained by reference to the photographic sequence for test 105 (figure 6, plate 1). Here we see that the nose of the mixed region begins to move with the initial wave (interpreted as a solitary wave in what follows) but it is soon left behind to be overtaken by the trough between the first and second waves, bringing the nose to rest. The next wave subsequently moves the nose forward, this sequence being repeated as other troughs and crests catch up to the nose of the mixed fluid.

Even more significant from the point of view of our present interpretation are the results shown in figure 7 (plate 1) and figure 8 (plate 2) for the largest value of ϕ (i.e.

Run no.	A	N	ϕ	Lower tangent point L/L_0	Lower tangent point tN	Upper tangent point L/L_0	Upper tangent point tN	n
105	1·0	1·15	0·36	2·20	5·68	4·39	16·11	0·71
106	1·0	1·13	0·36	2·52	7·13	4·23	16·58	0·66
107	1·05	1·00	0·38	2·53	8·64	5·50	22·63	0·89
108	1·05	1·00	0·38	1·67	4·20	4·19	16·99	0·70
110	1·05	0·84	0·38	2·28	6·08	4·92	18·06	0·76
111	1·1	0·80	0·39	2·58	6·24	5·59	17·54	0·78
112	1·05	0·65	0·38	2·16	6·05	5·13	19·38	0·77
113	1·1	0·60	0·39	1·95	4·85	4·74	16·06	0·76
167	1·0	0·88	0·50	5·00	1·55	15·67	5·57	0·89
170	1·0	0·97	0·50	3·67	1·14	14·53	5·67	0·89
96	0·56	0·92	0·34	3·14	9·80	8·27	34·52	0·79
97	0·56	0·92	0·34	3·00	9·43	7·09	31·87	0·75
98	0·56	0·67	0·34	2·60	7·34	6·50	28·10	0·70
101	0·58	1·01	0·36	2·07	7·82	5·15	26·50	0·83
103	0·59	1·17	0·38	2·02	6·81	4·36	22·90	0·65
104	0·59	1·15	0·39	1·63	4·70	3·79	32·27	0·55
69	0·27	1·75	0·29	1·53	5·96	6·27	93·49	0·53
72	0·30	1·78	0·30	?	?	?	?	0·76
75	0·28	1·60	0·28	1·33	3·99	2·59	12·76	0·65
78	0·32	1·48	0·32	4·17	24·24	5·49	42·87	0·48
82	0·29	1·30	0·30	1·53	5·31	2·52	11·54	0·64
86	0·29	1·22	0·28	2·45	10·13	5·09	31·99	0·60
114	0·31	0·82	0·20	1·43	4·82	2·25	16·85	0·38
115	0·31	0·78	0·20	1·59	5·61	2·09	12·31	0·43
116	0·33	0·60	0·22	1·49	5·27	2·60	17·77	0·49
117	0·33	0·57	0·22	1·53	5·42	2·46	15·23	0·50

TABLE 1. Exponents n and tangent points for all runs.

the mixed region fills the total height, H of the ambient stratification). The initial large-amplitude wave can be clearly seen carrying along (or being carried by) the mixed region. The maximum height of the nose moves exactly with the wave while the tip of the nose moves slightly slower because the length of the bulge decreases as the wave amplitude also decreases. In figure 7 the first wave can be seen as it leaves the nose of the mixed region behind, to be followed by the second and third waves. Figure 5 (f) plots the time history of this test and shows the passage of the three waves. Note, however, that the second and third waves have a much smaller effect on the motion of the mixed region as their amplitude decreased before their interaction with the nose. The character of the wave field (for another test) is shown in figure 9 where conductivity probe measurements taken just above the centre-line show two solitary waves followed by an almost constant amplitude wave train of frequency approximately equal to $0{\cdot}9N$.

The results of all the experiments are summarized in tables 1 and 2.† In figure 10 we plot mean n for several mean ϕ and A. Note that n increases for increasing ϕ and

† The tangent points are defined (after Wu 1969) as the points on the $\log L/L_0$ *vs.* $\log tN$ plot where a straight line describing the principal stage of collapse is tangent to the earlier (or later) stage.

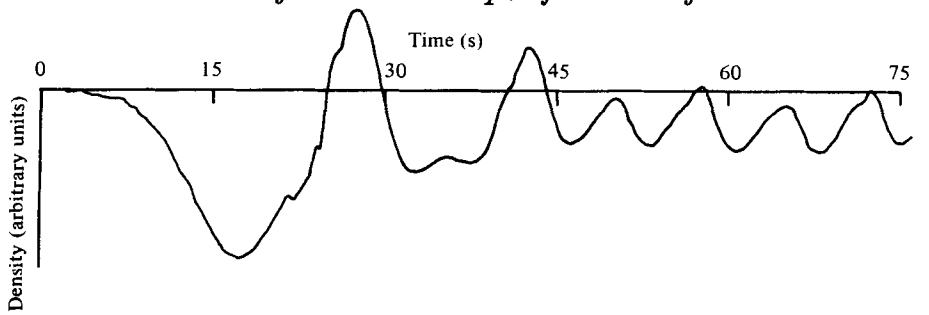

FIGURE 9. Conductivity probe output for an experiment with $\phi = 0{\cdot}5$, $A = 1$ and $N = 0{\cdot}93$ rad/s showing at least two mode two solitary waves plus a train of constant amplitude mode one waves (see figures 6 and 7 for the photographic evidence of the existence of these waves).

			Lower tangent		Upper tangent	
	n	ϕ	L/L_0	tN	L/L_0	tN
$\bar{A} = 1{\cdot}05 \pm 0{\cdot}08$						
Mean	0·75	0·38	2·24	6·12	4·84	17·92
Standard deviation	0·07	0·01	0·32	1·36	0·55	2·20
$\bar{A} = 0{\cdot}57 \pm 0{\cdot}03$						
Mean	0·71	0·36	2·41	7·65	5·86	27·86
Standard deviation	0·10	0·02	0·60	1·86	1·72	4·65
$\bar{A} = 0{\cdot}30 \pm 0{\cdot}04$						
Mean	0·55	0·26	1·89	7·96	3·48	28·31
Standard deviation	0·12	0·05	0·91	6·35	1·64	26·60

TABLE 2. Principal stage mean values and standard deviations of n, ϕ, A and tangent points.

appears to be independent of A, with the suggestion that for large enough ϕ, n will become unity. This would correspond to the case considered by Maxworthy (1980*b*) in which the nose of the mixed region was trapped within a solitary wave and moved with it. These results suggest that this ratio of h_0 to H determines the strength of the solitary waves produced. This is also supported by Whitham (1974), who shows that at least one solitary wave is produced and more solitary waves appear as a parameter describing the strength of the initial disturbance reaches critical values. For those values between the critical points a dispersive tail appears behind the last solitary wave.

Also of significance was the observation that the region always collapsed to a finite horizontal and vertical extent, i.e. did not continue to move indefinitely. This was due in part to the character of the initial density distribution in the mixed region and in part to mixing and diffusion along the boundaries during the collapse. The former consisted of a well-mixed centre with transition layers of order 0·5 cm thick at the top and bottom to match the outer linear profile. Mixing along the interface is minimal as the local Richardson number is relatively high and the Reynolds number is fairly low ($Re_0 \leqslant 4 \times 10^4$). Some mixing did occur owing to lifting the dam but was only important in the initial stage and was soon distorted and damped out. At the interface between the mixed region and the ambient fluid there must be some diffusion

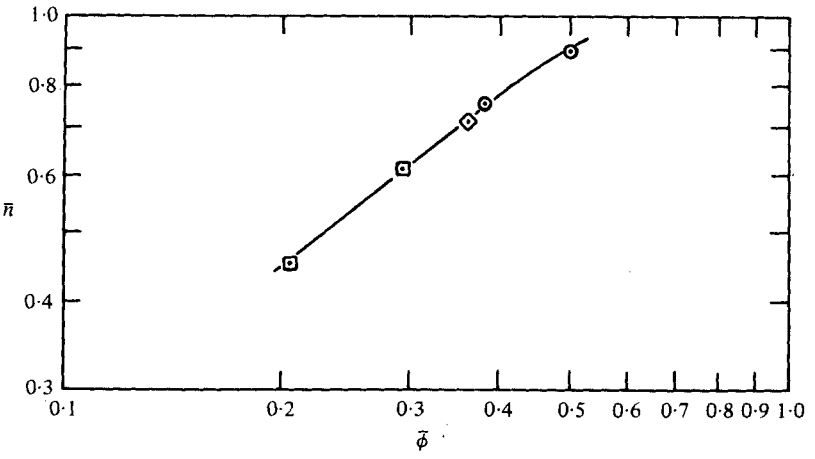

FIGURE 10. Mean value of exponent n *versus* mean ϕ with $\bar{A}$ as a parameter: ⊙, $\bar{A} = 1{\cdot}05$; ◇, $\bar{A} = 0{\cdot}57$; □, $\bar{A} = 0{\cdot}30$.

present to smear any sharp gradients. The total collapse process took several hours to complete and although the Schmidt number for salt in water is quite high ($Sc = \nu/D \simeq 10^3$) some diffusion must take place during the time scale of the collapse to further alter the density distribution in the mixed region. Thus the region collapses only until equilibrium is reached with the ambient density distribution and the final horizontal extent will be governed by the final density gradient within the mixed region. In the present experiments, the final vertical extent of the mixed region was between one half and two centimetres and always extended far down the tank, demonstrating that the initial region was mixed well enough. The result of these processes may also serve to explain the differences in the lower tangent points. As figure 2 shows, changes in the mixing ratio have a pronounced effect on the initial motion of the collapse.

The time of arrival of the first wave is presented in table 3 where $t_1 N$ is the dimensionless time of arrival at the six metre station and $t_2 N$ is the time of arrival at the twelve metre station. $\Delta t N$ is the difference of the two times, or the time of travel for the last six metres. For tests 110, 114 and 116 the wave travelled about 7 % slower in the last six metres than the mean for all the other tests. The data have systematic differences larger than the possible errors in measurement and yet there appears to be no correlation with any of the parameters ϕ, A and N. The wave speeds (computed for the first six metres of travel for several tests) as a function of N are plotted in figure 11 together with the long wave speed and the wave speed based on Wu's (1969) estimate for the wave frequency containing the majority of the wave energy. In all cases the time for the wave to travel the last six metres was longer than the travel time for the first six metres. This is somewhat surprising if we believe the previous work on this subject and interpret these as linear waves with no phase speed dependence on amplitude. The waves are however subject to dissipation, mainly at the side walls and our observation suggests that the decrease in wave speed is due to a decrease in wave amplitude and hence that nonlinear effects cannot be ignored.

When the waves reached the wave trap they were not destroyed as was expected

Run no.	t_1N	t_2N	ΔtN
103	127·0	262·2	135·2
104	123·6	256·5	132·9
106	126·3	263·3	137·0
107	116·9	250·7	133·8
108	122·7	257·0	134·3
110	139·7	282·4	142·7
111	126·3	262·3	136·0
113	131·2	268·2	137·0
114	134·2	277·3	143·1
115	130·9	268·1	137·2
116	131·8	278·1	146·3
117	130·0	254·9	124·9
Mean	128·4	265·1	136·7
Standard deviation	5·9	10·0	5·6

TABLE 3. Time of arrival of the first wave at 6 and 12 m downstream.

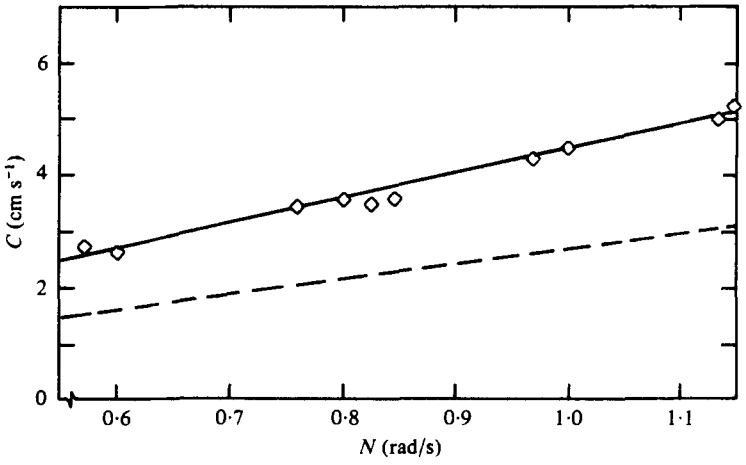

FIGURE 11. Phase speed C of the first wave produced by the collapse versus N. Comparison with the long wave speed of a mode two wave (——) and the mode two wave speed for $\omega = 0{\cdot}8N$ at which Wu (1969) places most of the wave energy (– – –).

from the calculations based on Wu's (1969) observations but the waves appeared to change modal structure during the time spent interacting with the wave trap. As mentioned above, we believe that the waves produced by the collapse are not all linear waves and hence the wave trap can not absorb these waves as it was designed according to linear theory. All of these observations and particularly a perusal of the distortions created by the waves (figures 6–8) strengthens our convinction that at least one solitary wave (the first) is formed by such a collapse and that the waves following may either be more solitary waves or a dispersive wave train, depending on the intensity of the initial disturbance.

5. Discussion and conclusions

An analytical model has been presented for the motion of a collapsing mixed region, valid for small times following the release from rest. Unlike previous analyses, the present one attempts to model the kinetic energy in the flow field external to the mixed region. The results are in reasonable agreement with experimental data up to $tN = 2{\cdot}5$ for $A = 1$. They diverge after that but appear to be an improvement over previous results. The numerical results of Dugan *et al.* (1976) show undulations on, the interface between the mixed region and the exterior fluid. These undulations appear to be due to an instability of the Kelvin–Helmholtz type. The experimental results of Wu (1969) and the present study do not show the development of any such instability on the interface. As mentioned above, the removal of the dam caused some disturbance at the nose but this was quickly damped out. Wu (1969) has shown that the interface Richardson number ($Ri_i = -(g/\rho)(\partial\rho/\partial z)(\partial u/\partial z)_i^{-2}$) was always greater than $\frac{1}{2}$. With this in mind it is not surprising that the interface is stable in the experiments. As was pointed out above, the numerical results of Dugan *et al.* (1976) for an infinitesimally thin interface also indicate a higher acceleration than is found in the experiments and this most likely results in the instability of the interface shown there. It has been suggested that these undulations may generate the internal waves found in the experiments. The experiments of Wu (1969), the theoretical investigations of Mei (1969) and others have demonstrated that linear internal waves can be generated quite effectively by the advancing nose of the mixed region alone. For any analytical solution to agree well with the experiment, the energy lost to the internal wave field must be included in the energy balance. The experiments have revealed that there is a considerable amount of energy in the internal wave field and that most of this energy is deposited during the initial stage of collapse.

The interpretation of these results has been influenced by those presented in Maxworthy (1980*b*). In that paper we found that the initial wave produced by a collapse was invariably a solitary wave followed by more solitary waves or a train of weakly dispersive waves (if the initial disturbance was weak). The major difference between the two sets of experiments is that in Maxworthy (1980*b*) the vertical scale of the mixed region was always larger than that of the ambient stratification. In the present experiment the mixed region is embedded in the ambient stratification and has a vertical length scale equal to or smaller than that of the ambient stratification. This results in the generation of weak waves and because of this the solitary wave characteristics of at least the first wave have not been noted before. Furthermore, an analysis of the linear wave motions to be expected from such a collapse (Amen 1978) does not agree in any respect with the present observations. The appearance of solitary waves is also consistent with known facts about their generation in other circumstances [see Whitham (1974), for example]. It has been shown that in physical systems that obey a Korteweg–de Vries equation (as in the present case) such a collapse generates at least one solitary wave and that as the size of the collapsing region becomes larger, solitary waves appear in 'quantum jumps'. A dispersive wave train appears if the condition for an integral number of waves is not exactly satisfied.

It appears from Wu's (1969) published results that only one solitary wave plus a dispersive tail was produced by his weak disturbance. His experiment had $\phi = 0{\cdot}125$ and hence this resulted in a relatively weak disturbance and for disturbances of this

type one expects at most one solitary wave, followed by a dispersive wave train. The solitary wave in this case will quickly leave the mixed region behind and will effect the motion of the nose only in the very initial stage. Linear wave theory will then be applicable and has provided good agreement with the wave motion seen in Wu's (1969) experiment. In the present experiments $\phi \geqslant 0{\cdot}2$ and these represent a class of stronger disturbances. When the vertical length scales of the disturbance and the ambient stratification are comparable, more solitary waves are expected (Whitham 1974) and hence a stronger (or more prolonged) interaction between the solitary wave motion and that of the collapsing mixed region. It is felt that these conditions more closely resemble those found in the ocean.

In our case we believe that the pulsing of the nose of the mixed region, a condition not observed by Wu, can be explained by the passage of a number of solitary waves past it after it has been left behind by the leading wave. These results suggest that a theoretical explanation in terms of a balance between inertia and buoyancy forces is probably only of use in very restrictive circumstances of which Wu's are one example.

This mechanism has also been used to describe the generation of solitary waves in a number of natural systems including the Jovian Great Red Spot (Maxworthy, Redekopp & Weidman 1978), internal waves over the continental shelf (Maxworthy 1979, 1980; Smith & Farmer 1977), atmospheric internal waves (Christie, Muirhead & Hales 1978), etc., and we anticipate discovery of further examples in the future.

The authors wish to acknowledge the support of the office of Naval Research during the course of this research. Casey de Vries built much of the apparatus and together with Setsuko Odo helped run the experiments. Their help is gratefully acknowledged.

REFERENCES

AMEN, R. 1978 The collapse of a two-dimensional mixed region in a density stratified fluid. M.S. thesis, University of Southern California.

BELL, T. H. & DUGAN, J. P. 1974 Model for mixed region collapse in a stratified fluid. *J. Engng Math.* **8**, 241–248.

BROWAND, F. K. & WINANT, C. D. 1972 Blocking ahead of a cylinder moving in a stratified fluid: an experiment. *Geophys. Fluid Dyn.* **4**, 29–53.

CHRISTIE, D. R., MUIRHEAD, K. J. & HALES, A. L. 1978 On solitary waves in the atmosphere. *J. Atmos. Sci.* **35**, 805–825.

DUGAN, J. P., WARN-VARNAS, A. C. & PIACSEK, S. A. 1976 Numerical results for laminar mixed region collapse in a density stratified fluid. *Comp. Fluids* **4**, 109–121.

HARTMAN, R. J. & LEWIS, H. W. 1972 Wake collapse in a stratified fluid: linear treatment. *J. Fluid Mech.* **51**, 613–618.

HINDMAN, C. L. 1974 Wake collapse in a stratified fluid: linear internal wave generation problem. Ph.D. thesis, University of Colorado.

KAO, T. W. 1976 Principal stage of wake collapse in a stratified fluid: two dimensional theory. *Phys. Fluids* **19**, 1071–1074.

LONG, R. R. 1970 A theory of turbulence in stratified fluids. *J. Fluid Mech.* **42**, 349–365.

MANINS, P. C. 1976*a* Intrusion into a stratified fluid. *J. Fluid Mech.* **74**, 547–550.

MANINS, P. C. 1976*b* Mixed region collapse in a stratified fluid. *J. Fluid Mech.* **77**, 177–183.

MAXWORTHY, T. 1979 A note on the internal solitary waves produced by tidal flow over a three dimensional ridge. *J. Geophys. Res.* (in the press).

MAXWORTHY, T. 1980 On the formation of nonlinear internal solitary waves from the gravitational collapse of mixed regions in two and three dimensions. *J. Fluid Mech.* **96**, 47–64.

MAXWORTHY, T. & BROWAND, F. K. 1974 Experiments in rotating and stratified flows: oceanographic application. *Ann. Rev. Fluid Mech.* **7**, 273–305.

MAXWORTHY, T., REDEKOPP, L. G. & WEIDMAN, P. 1978 On the production of planetary solitary waves: applications to the Jovian atmosphere. *Icarus* **33**, 338–409.

MEI, C. C. 1969 Collapse of a homogeneous fluid in a stratified fluid. *Proc. of the 12th Int. Cong. Appl. Mech.* (ed. M. Hetenyi & W. G. Vincenti). Springer.

MERRITT, G. E. 1974 Wake growth and collapse in a stratified flow. *A.I.A.A. J.* **12**, 940–949.

OSTER, G. 1965 Density gradients. *Sci. Am.* **213**, 70–76.

PAO, H. P. 1974 Collapse of a two dimensional mixed region in a stratified fluid. *Bull. Am. Phys. Soc.* **19**, 1164.

SCHOOLEY, A. H. & HUGHES, B. A. 1972 An experimental and theoretical study of internal waves generated by the collapse of a two-dimensional mixed region in a density gradient. *J. Fluid Mech.* **51**, 159–175.

SCHOOLEY, A. H. & STEWART, R. W. 1963 Experiments with a self-propelled body submerged in a fluid with a vertical density gradient. *J. Fluid Mech.* **15**, 83–96.

SMITH, J. D. & FARMER, D. M. 1977 Non-linear internal waves and internal hydraulic jumps in a fjord. In *Geofluiddynamic Wave Mechanics*, pp. 42–53. University of Washington, Seattle.

WESSEL, W. R. 1969 Numerical study of the collapse of a perturbation in an infinite density stratified fluid. *Phys. Fluids Suppl.* **12**, II171–II176.

WHITHAM, G. B. 1974 *Linear and Nonlinear Waves*. Wiley-Interscience.

WOODS, J. D. 1968 Wave-induced shear instability in the summer thermocline. *J. Fluid Mech.* **32**, 791–800.

WU, J. 1969 Mixed region collapse with internal wave generation in a density-stratified medium. *J. Fluid Mech.* **35**, 531–544.

WUNSCH, C. 1968 On the propagation of internal waves up a slope. *Deep Sea Res.* **25**, 251–258.

YOUNG, J. A. & HIRT, C. W. 1972 Numerical calculation of internal wave motions. *J. Fluid Mech.* **56**, 265–276.

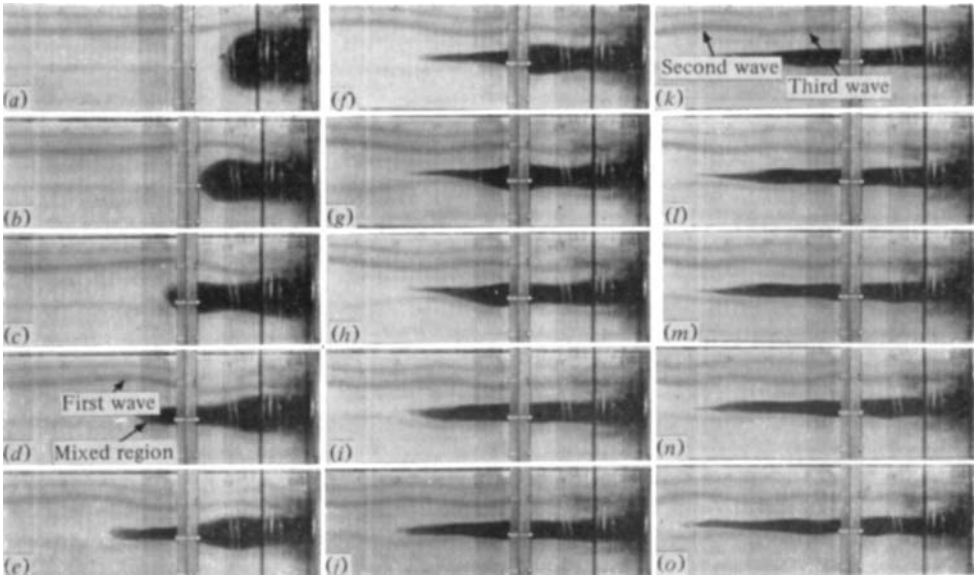

FIGURE 6. Photographic sequence showing the appearance of the mixed region at various times. Time increases downwards from the top left-hand picture. Values of tN for each picture are: (*a*) 3·04; (*b*) 5·68; (*c*) 7·97; (*d*) 10·38; (*e*) 12·67; (*f*) 14·96; (*g*) 17·37; (*h*) 18·63; (*i*) 22·19; (*j*) 24·48; (*k*) 27·12; (*l*) 30·44; (*m*) 31·76; (*n*) 33·19; (*o*) 35·94. In particular note the passage of internal waves past the nose of the mixed region which account for its motion, as shown in figure 5(*e*). $A = 1{\cdot}0$, $\phi = 0{\cdot}36$, $N = 1{\cdot}15$ rad/s.

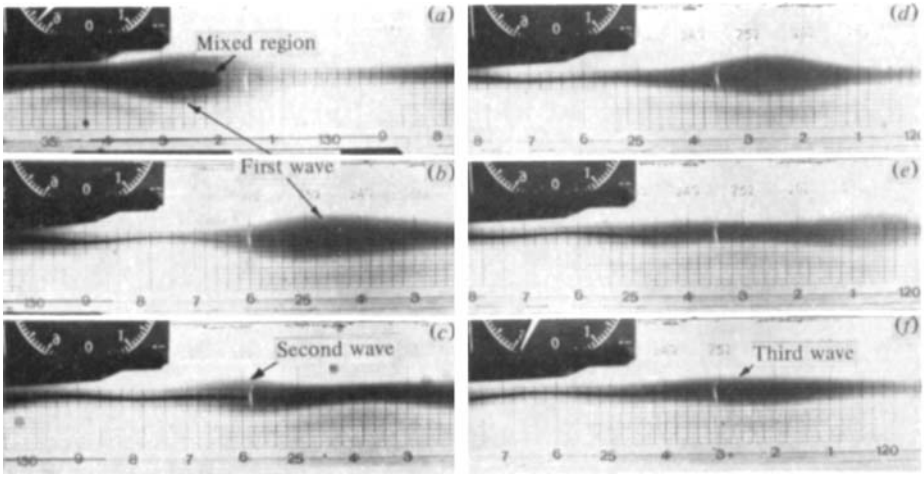

FIGURE 7. Sequence showing passage of internal solitary waves past the mixed fluid. Values of tN are: (*a*) 3·90; (*b*) 5·67; (*c*) 6·59; (*d*) 7·52; (*e*) 8·08; (*f*) 8·87. In (*b*) the first wave leaves the mixed region behind to be followed by a second in (*d*) and a third in (*f*). $A = 1{\cdot}0$, $\phi = 0{\cdot}5$, $N = 0{\cdot}97$ rad/s.

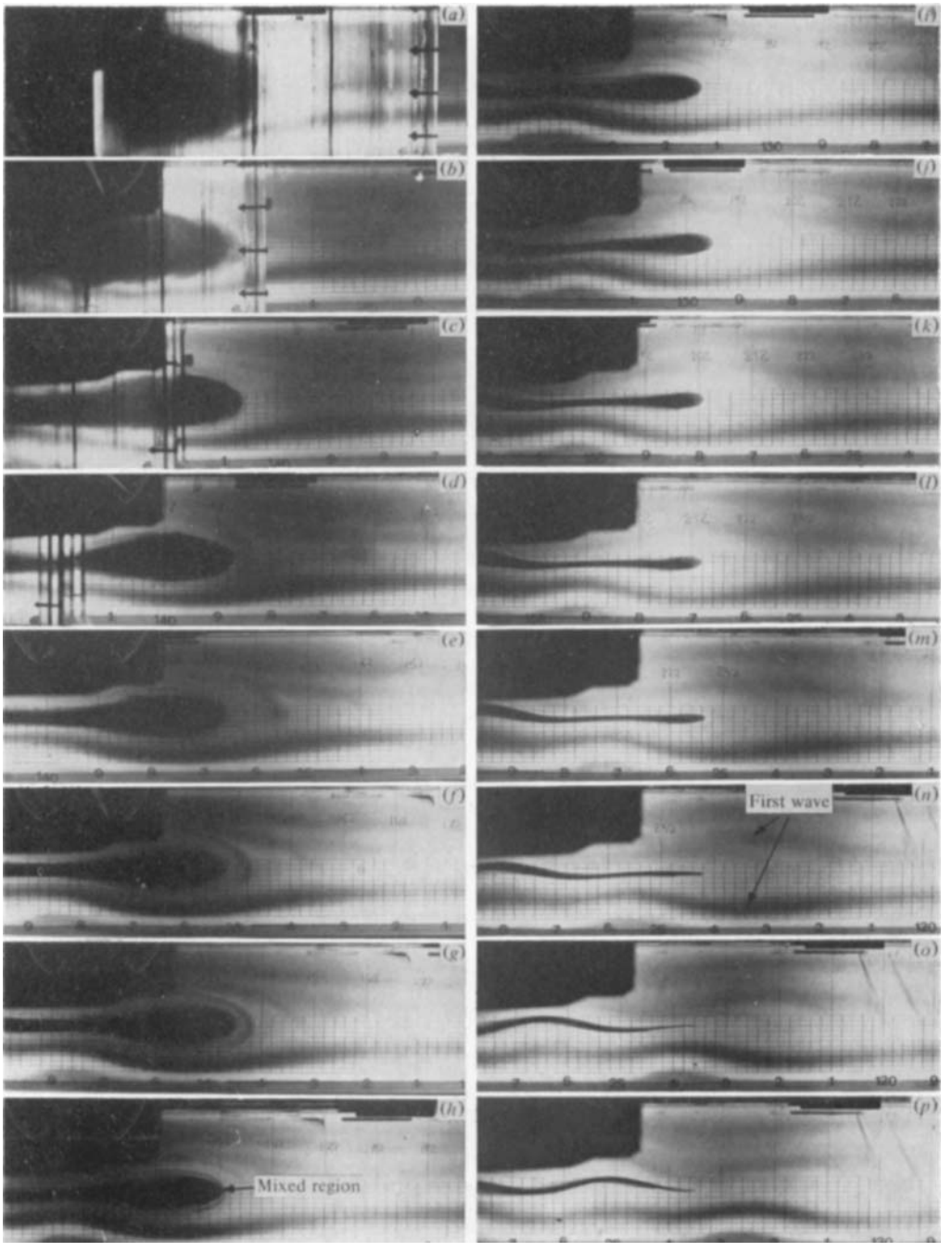

FIGURE 8. Photographic sequence of collapse for $\phi = 0{\cdot}5$, $A = 1{\cdot}0$ and $N = 0{\cdot}88$ rad/s. Values of tN are: (*a*) 0·45; (*b*) 1·09; (*c*) 2·02; (*d*) 2·51; (*e*) 2·85; (*f*) 3·04; (*g*) 3·79; (*h*) 4·25; (*i*) 4·66; (*j*) 4·95; (*k*) 5·37; (*l*) 5·75; (*m*) 6·14; (*n*) 6·44; (*o*) 6·79; (*p*) 7·12. Note that the first wave and the mixed region move together initially (see figure 5*f*).